analytical chemistry

Editors' Highlight

pubs.acs.org/ac

Interactions of Hemoglobin and Myoglobin with Their Ligands CN^-, CO, and O_2 Monitored by Electrospray Ionization-Mass Spectrometry

Modupeola A. Sowole, Stephanie Vuong, and Lars Konermann*

Department of Chemistry, The University of Western Ontario, London, Ontario N6A 5B7, Canada

ABSTRACT: Electrospray ionization (ESI)-mass spectrometry (MS) can provide information on protein−ligand interactions via detection of the corresponding complexes as gaseous ions. Unfortunately, some systems are prone to dissociation upon transfer into the gas phase. The reversible oxygen binding to hemoglobin (Hb) has been extensively studied in solution using a wide range of biophysical techniques. In addition to O_2, ferrous (Fe^{II}) Hb can bind CO. High affinity interactions with CN^- are limited to the ferric (Fe^{III}) state. In analogous fashion, CN^-, CO, and O_2 bind to myoglobin (Mb). It remains unclear whether any of these ligand-bound forms can be observed by ESI-MS. In this work we demonstrate the successful detection of MbCN, while MbCO and MbO_2 do not survive under ESI-MS conditions. Control experiments suggest that an older report of "MbO_2" detection by ESI-MS may involve the misassignment of oxidation artifacts formed under corona discharge conditions. The situation is more favorable for ESI-MS studies on Hb. The most intense signal in the HbCN mass distribution corresponds to the expected complex with four cyanide moieties bound. Ligand loss during ESI-MS is around 20%. HbCO is detectable as well, albeit with a more noticeable level of ligand dissociation (~50%) which produces the 2CO-bound state as the highest intensity ion in the spectrum. In addition, our data suggest that low levels of HbO_2 can survive the transition into the gas phase, evident from +64 Da and +128 Da signals that can be assigned to Hb carrying two and four oxygen molecules, respectively. The application of collisional activation induces neutral ligand loss for all three Hb derivatives. It appears that this is the first report on the detection of MbCN, HbCO, and HbO_2 in the gas phase. We hope that this work will pave the way towards future spectroscopic investigations of desolvated Mb and Hb, complementing the extensive literature on CN^-, CO, and O_2 bound globins in the condensed phase.

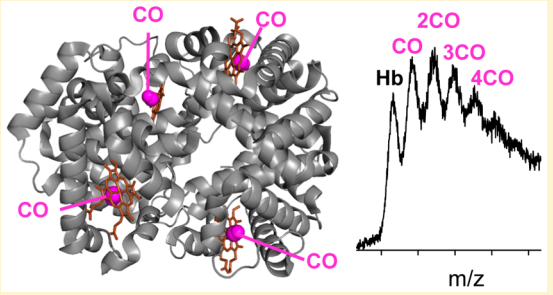

Electrospray ionization (ESI)-mass spectrometry (MS)[1] has become a widely used tool for interrogating protein−protein and protein−ligand interactions. The possibility to transfer intact biomolecular assemblies into the gas phase by "native" ESI[2−7] (or nanoESI[8]) provides information on binding stoichiometries via simple mass measurements. Electrosprayed complexes can be further interrogated, e.g., by conducting dissociation studies[9−12] or ion mobility experiments.[13−15] Unfortunately, in some cases the transition from solution into the gas phase causes the disruption of protein−ligand interactions.[16,17] Nonspecific adduction can take place as well.[18,19] Strategies have been developed to address these issues,[16,17] but the viability of ESI-MS binding studies nonetheless has to be assessed on a case-by-case basis.

Hemoglobin (Hb) serves as oxygen carrier in red blood cells.[20,21] In the physiologically active protein, each of the four subunits contains a ferrous heme iron (Fe^{II}) that is coordinated by a proximal histidine. Oxygen binding takes place at the opposite face of the heme, where O_2 can occupy the remaining coordination site while also forming a H-bond with a distal histidine.[22−25] The oxygen-saturated protein (with four O_2 bound) is referred to as HbO_2. The allosteric nature of oxygen binding to Hb and the associated structural changes of the $(\alpha\beta)_2$ quaternary structure continue to be a topic of research.[25−30] Similarly, the changes in iron and oxygen electron configuration during binding remain under investigation.[24,31,32]

Fe^{II} Hb can also bind ligands other than O_2; the interaction with CO is of particular physiological relevance.[33] The CO binding affinity of Fe^{II} Hb is ~250 times higher than its O_2 affinity.[24] In HbCO the four CO molecules interact with heme in a $Fe^{II}\cdots$CO orientation, rather than $Fe^{II}\cdots$OC.[34] CO is a colorless gas that can form as combustion byproduct; it is present in car exhaust and tobacco smoke. The HbCO level in smokers can be as high as 15%, compared to 1−3% in nonsmokers.[35] Excessive HbCO formation leads to hypoxia and death.

Auto-oxidation of Fe^{II} HbO_2 generates Fe^{III} Hb (metHb) that has the distal heme ligation sites occupied by water.[36] Fe^{III} Hb formation can take place under physiological stress[34] as well as during protein isolation, storage, and lyophilization.[37] Fe^{III} Hb is incapable of O_2 binding, but it has an extremely high affinity for CN^-. Quasi-irreversible $Fe^{III}\cdots$CN binding at the four hemes leads to water displacement from the distal sites.[21,38] HbCN is important for spectroscopic and crystallographic studies.[21,34]

Received: July 3, 2015
Accepted: September 1, 2015
Published: September 1, 2015

DOI: 10.1021/acs.analchem.5b02506
Anal. Chem. 2015, 87, 9538−9545

Myoglobin (Mb) is a monomeric oxygen storage protein that exhibits a tertiary structure very similar to that of the Hb subunits.[39] Ligand interactions in Mb are analogous to those discussed above for Hb.[21] Oxygen binding to Fe^{II} heme generates MbO_2, while carbon monoxide exposure yields MbCO. Mb auto-oxidation produces water-bound Fe^{III} Mb[39] that readily converts to MbCN in the presence of CN^-.[38,40] A key difference between Hb and Mb is the noncooperative binding mechanism of the latter, giving rise to O_2 binding profiles that are hyperbolic rather than sigmoidal.[41]

From the early 1990s[42] to the present day,[43] heme proteins have played a central role for the development of native ESI-MS as a tool for probing biomolecular interactions. A considerable number of studies have focused on heme binding to Mb,[44−48] as well as subunit interactions in Hb.[37,49−53] Surprisingly, very few native ESI-MS reports focused on globin binding to CN^-, CO, and O_2. This is in striking contrast to other biophysical techniques which have exhaustively been applied for studying these complexes.[21,25−30,54,55]

ESI-MS studies on globin complexes with CN^-, CO, and O_2 face several challenges. (i) Mb and Hb are designed for facile O_2 release upon exposure to a deoxygenated environment. Thus, it can be envisioned that rapid O_2 loss will take place upon transferring the proteins into the vacuum of the mass spectrometer. Indeed, several ESI-MS studies on MbO_2 and HbO_2 found no evidence of oxygen retention.[37,44,47,53] (ii) As discussed above, the ligand binding properties depend critically on the heme oxidation state.[21] The operation of an ESI source is associated with charge-balancing redox processes.[56−58] In positive ion mode, this can lead to inadvertent $Fe^{II} \rightarrow Fe^{III}$ heme oxidation,[59,60] while $Fe^{III} \rightarrow Fe^{II}$ reduction may take place in negative ion mode.[44] (iii) Side chain oxidation can give rise to multiple +16 Da covalent modifications that might be mistaken for O_2 binding. Such oxidation events have been shown to take place during storage,[37] at the metal−liquid interface of the ESI emitter,[61,62] or they can arise from reactive oxygen species formed under corona discharge conditions within ESI droplets or in the gas phase.[63−65]

Interestingly, one 1994 ESI-MS study reported the observation of a Mb + 32 Da species that was interpreted as MbO_2, i.e., the proper heme-O_2 bound form of the protein.[66] It is surprising that there appear to be no follow-up investigations that confirmed this finding or extended it to Hb. Partial retention of CN^- to Fe^{III} Hb was demonstrated in one instance.[64] As far as we are aware, there are no reports of ESI-MS experiments on CO-bound globins. Thus, there remain considerable gaps in the understanding of Mb and Hb interaction with their physiologically relevant ligands under ESI-MS conditions. The current work addresses this issue by applying ESI-MS to the CN^-, CO, and O_2 bound forms of Mb and Hb. Our results suggest that the "MbO_2" observed previously[64] may have been an oxidation artifact. Under the conditions of the current work, MbCN is the only bound Mb species that can be observed in the gas phase. The situation is more favorable for Hb, where we demonstrate the detection of ligand-bound HbCN and HbCO. Our data suggest that even for HbO_2 a low level of ligand retention is possible. To our knowledge, several of the globin complexes reported here have not previously been observed by ESI-MS.

EXPERIMENTAL SECTION

Sample Preparation. Ammonium acetate, sodium dithionite, potassium ferricyanide, and horse heart metMb were purchased from Sigma (St. Louis, MO). KCN was from Caledon (Georgetown, ON, Canada). Bovine Fe^{II} HbO_2 was isolated from fresh blood.[37] Fe^{II} HbCO was prepared by bubbling HbO_2 solution with carbon monoxide gas for 1 h in a fume hood.[21] MetHb was prepared by exposure of Fe^{II} HbO_2 to ferricyanide. The latter was subsequently converted to Fe^{III} HbCN by addition of KCN.[37,67] Similarly, Fe^{III} MbCN was produced by KCN addition to horse heart metMb. Fe^{II} MbO_2 was generated by reduction of metMb using dithionite as described.[67] Subsequent CO bubbling yielded Fe^{II} MbCO. Aqueous solution used for ESI-MS contained 10 mM ammonium acetate at pH 7. Protein concentrations were 10 μM for Mb and 60 μM for Hb.

Mass Spectrometry. All measurements were conducted on a Synapt HDMS time-of-flight mass spectrometer (Waters, Milford, MA). Two types of ion sources were employed. Regular ESI-MS experiments employed the standard Z-spray source at a capillary voltage of 2.8 kV (unless noted otherwise) and a desolvation gas flow rate of 800 L h^{-1}. Solutions were infused at 5 μL min^{-1}. NanoESI was conducted using gold-coated emitters made from borosilicate glass capillaries (BF 100-78-10, Sutter, Novato, CA) using a microcapillary puller (Sutter PC-84). Capillaries were coated using a Hummer VI Sputtering System (Union City, CA) operated at a N_2 plasma pressure of 100 mTorr at 10 mA for 5 min. The nanoESI source was operated at 1.5 kV and the flow was assisted by a very low N_2 pressure of 0.05 bar. The resulting solution flow rate was ~40 nL min^{-1}, as determined gravimetrically. The source backing pressure was adjusted to 5 mbar by a SpeediValve on the scroll pump. The appearance of the mass spectra was found to be largely independent of the ion source used. Unless noted otherwise, the data shown in the figures below were obtained by nanoESI. For positive ESI, the instrument settings were as follows: source 80 °C, desolvation 100 °C, sample cone voltage 5 V, extraction cone 2 V, cone gas flow 50 L h^{1-}, trap collision energy 6 V, transfer collision energy 4 V, trap wave velocity 300 ms^{-1}, and trap wave height 0 V. The trap bias was set at 4 V for Mb and 0 V for Hb. The same settings were used in negative ion mode, except that the trap wave height was changed to 0.5 V. Adjusting the instrument conditions in this way provides a minimum of analyte activation along the ion path in order to promote the retention of weakly bound ligands. The downside of using these gentle conditions is a relatively poor ion transmission that reduces spectral S/N ratios. In selected experiments, the protein ions were deliberately exposed to collisional activation, using Ar as collision gas. For MS/MS on Hb the transfer collision energy was raised to 40 V. MS/MS experiments on Mb were conducted by setting the trap collision energy to 35 V. NaI cluster ions were used for mass calibration. All spectra depicted in this work are shown without any smoothing to ensure the absence of data processing artifacts.

RESULTS AND DISCUSSION

UV−Visible Absorption Spectra. Prior to conducting ESI-MS experiments, we used UV−vis absorption spectroscopy to test whether the CN^-, CO, and O_2 globin derivatives used in this work had the expected bulk solution properties. Different heme oxidation states and ligand binding properties give rise to characteristic optical signals (Figure 1). In addition to the Soret region (around 400 nm), the range between 500 and 600 nm is of interest. Here, Fe^{II} heme exhibit two bands around 540 nm ("β") and 580 nm ("α"), as seen for the CO and O_2 forms of

DOI: 10.1021/acs.analchem.5b02506
Anal. Chem. 2015, 87, 9538−9545

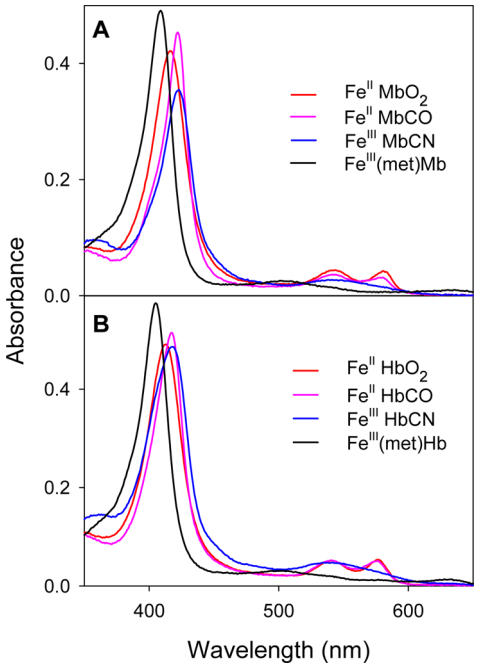

Figure 1. UV–vis absorption spectra of (A) four different Mb derivatives and (B) four different Hb derivatives in aqueous solution containing 10 mM ammonium acetate at pH 7. In addition to the CN^-, CO, and O_2 derivatives this figure also shows the spectra of metMb and metHb.

Mb and Hb. This distinct double-peak is absent for the Fe^{III} heme of the CN^- bound forms as well as metMb and metHb. All spectral maxima of the UV–vis data in Figure 1 agree with the literature[21] to within 1 nm or less, thereby confirming the fidelity of the samples used.

ESI-MS Analysis of Mb–Ligand Interactions. Mass spectra obtained by nanoESI-MS of MbCN, MbCO, and MbO_2 in positive ion mode are dominated by protein ions in the 9+ and 8+ charge states, consistent with a tightly folded solution conformation (Figure 2A–C).[45] Examination of the MbCN spectrum reveals that the protein largely retains its cyano ligand; the 9+ and 8+ peaks are split between protonated and K^+-adducted MbCN. The latter is consistent with the use of KCN for sample preparation. Only a small fraction (~10%) of the protein ions is in the CN-free state (Figure 2D). In contrast, there is no evidence of ligand retention for MbCO and MbO_2 (Figure 2E,F), despite tuning the instrument conditions to be as gentle as possible (see Experimental Section).

MS/MS was conducted by selecting the highest signal in the 9+ range as the precursor ion. The goal of these experiments was to determine the heme oxidation state in the gas phase. Free Fe^{II} heme has an overall charge of zero; collisional dissociation can thus proceed as neutral loss or as loss of a protonated (singly positively charged) species (m/z 617.2). In contrast, Fe^{III} heme has an intrinsic positive charge such that it will appear as the 1+ ion at m/z 616.2.[44,47] The tandem mass spectrum of Figure 2G reveals that MbCN undergoes

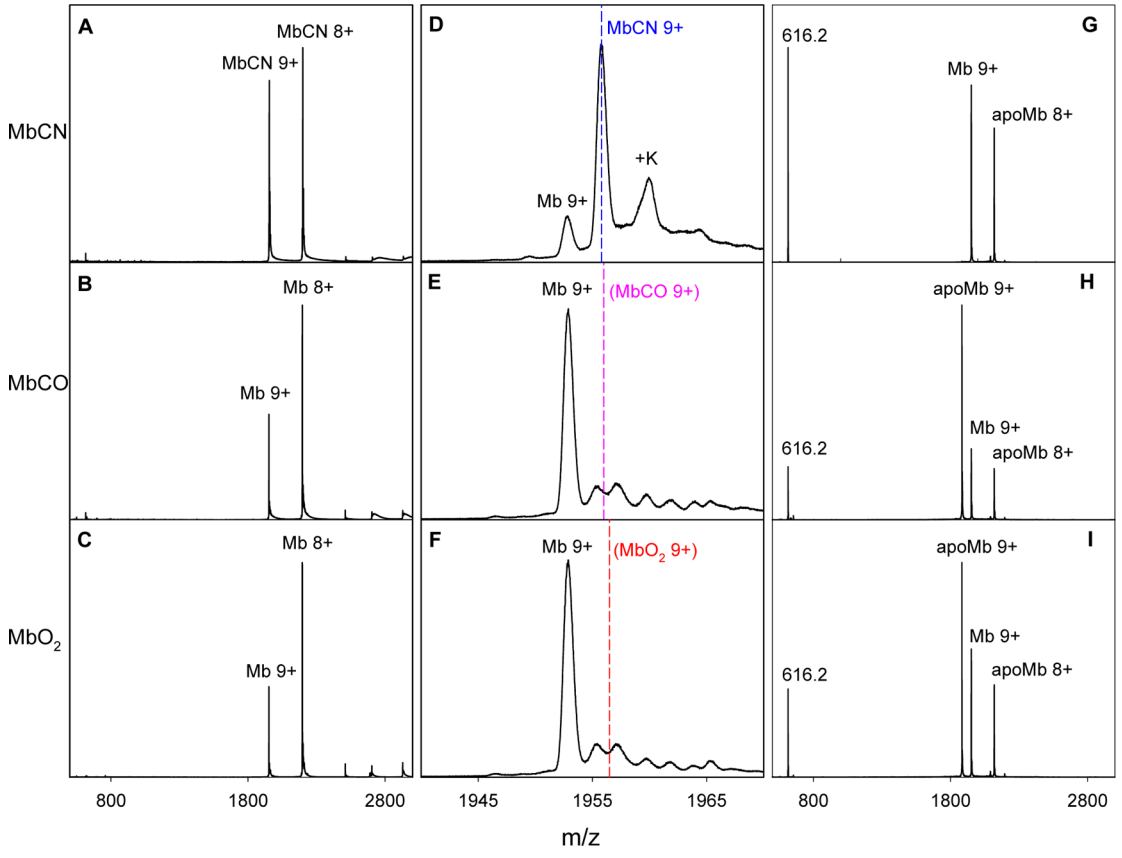

Figure 2. Mass spectra obtained in positive ion mode by exposing Fe^{III} MbCN (first row), Fe^{II} MbCO (middle row), and Fe^{II} MbO_2 (bottom row) to nanoESI conditions. Complete spectra are depicted in panels A–C. Panels D and E show close-ups of the 9+ region. Dashed lines indicated the expected positions of ligand bound protein ions. Panels G–I show tandem mass spectra, obtained for the precursor ions MbCN 9+ (G) and Mb 9+ (H, I).

DOI: 10.1021/acs.analchem.5b02506
Anal. Chem. 2015, 87, 9538–9545

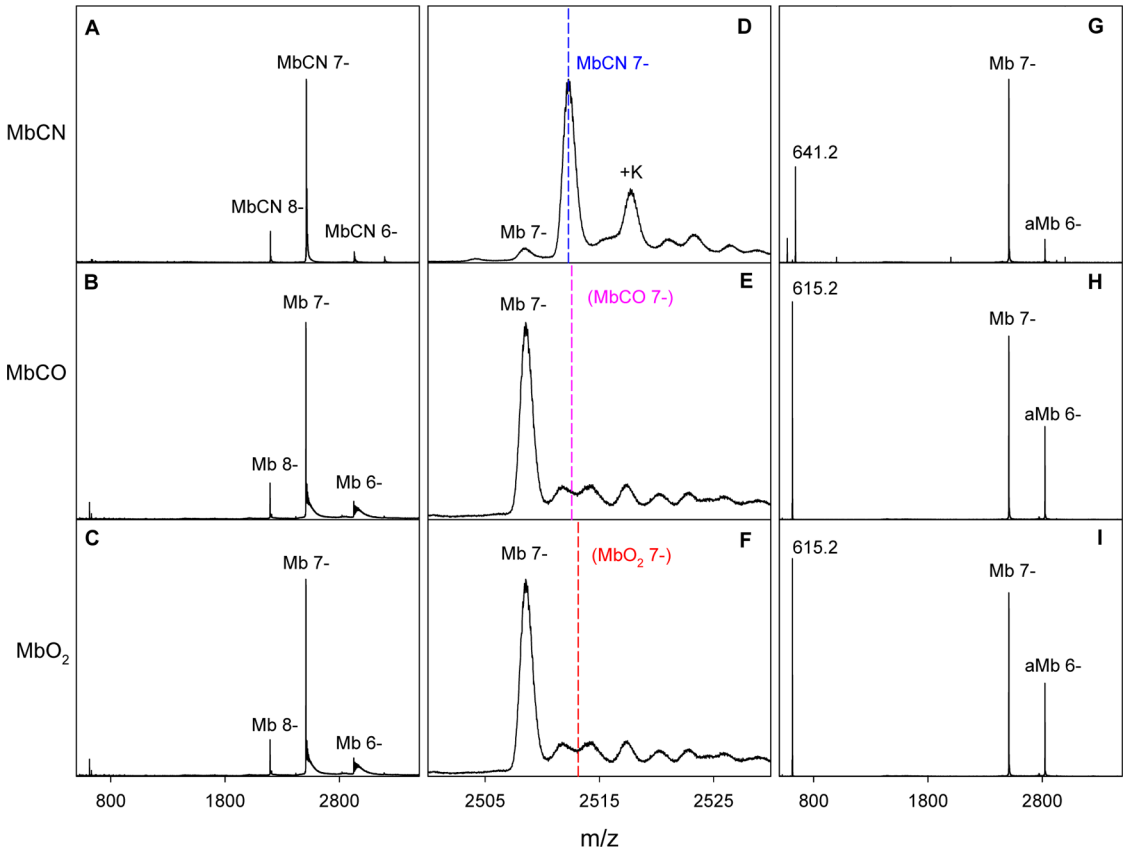

Figure 3. Mass spectra obtained in negative ion mode by exposing Fe^{III} MbCN (first row), Fe^{II} MbCO (middle row), and Fe^{II} MbO_2 (bottom row) to nanoESI conditions. Complete spectra are depicted in panels A–C. Panels D and E show close-ups of the 7− region. Panels G–I show tandem mass spectra, obtained for the precursor ions MbCN 7− (G) and Mb 7− (H, I).

dissociation according to $MbCN^{9+} \rightarrow [Fe^{III}\ heme]^{+} + apoMb^{8+} + HCN$. In other words, the Fe^{III} oxidation state of the heme remained unchanged during ESI-MS analysis of MbCN. MS/MS of MbCO and MbO_2 generates product ions that arise from two parallel reactions, $Mb^{9+} \rightarrow [Fe^{III}\ heme]^{+} + apoMb^{8+}$ and $Mb^{9+} \rightarrow [Fe^{II}\ heme]^{0} + apoMb^{9+}$ (Figure 2H,I). The first of these reactions highlights the partial oxidation of Fe^{II} Mb to Fe^{III} Mb during ESI,[44,59,60] consistent with the known fact that charge balancing processes in positive ion mode provide an oxidizing environment within the emitter.[56−58]

The data of Figure 2 suggest that ESI-induced $Fe^{II} \rightarrow Fe^{III}$ oxidation might be a contributing factor to the loss of CO and O_2 from Mb, keeping in mind that only ferrous heme is capable of interacting with these two ligands.[21] We examined this possibility by conducting negative ion nanoESI-MS measurements which provide a reducing environment[56−58] (Figure 3). MS/MS confirms that Fe^{II} Mb does not change its oxidation state in negative ion mode, evident from the observation of singly deprotonated Fe^{II} heme at m/z 615.2 (Figure 3H,I). The ligand binding behavior of gaseous Mb in negative ion mode (Figure 3A–F) was identical to that of Figure 2, i.e., CN^{-} was retained, while MbCO and MbO_2 were not detectable. It is concluded that the ligand loss experienced by MbCO and MbO_2 under ESI-MS conditions is not due to electrochemically induced changes in heme oxidation state. For completeness, it is noted that the m/z 641.2 signal generated by collisional activation of MbCN 7- corresponds to $[Fe^{III}\ heme + CN - H]^{-}$ (Figure 3G). Thus, we found no evidence of $Fe^{III} \rightarrow Fe^{II}$ reduction for MbCN in negative ion ESI, although this process can take place for metMb.[44]

ESI-Mediated Covalent Modifications. Considering the labile nature of the protein–ligand interactions in MbO_2, it is perhaps not surprising that we were unable to observe this species by ESI-MS. However, an early triple quadrupole positive ion ESI-MS study reported the detection of a Mb + 32 Da adduct signal that was attributed to the protein-heme···O_2 complex.[66] It seems peculiar that (to our knowledge) there have been no follow-up reports of O_2-bound heme proteins in the intervening 20 years. The question arises whether the "MbO_2" ions seen in that work[66] could represent an artifact, rather than a complex of Mb with O_2. To highlight a possible source of such artifacts, Figure 4 illustrates the effects of raising the ESI capillary voltage on a Z-spray ion source from the standard value of 2.8 kV to 5.0 kV during infusion of MbO_2. Standard conditions generate Mb ions that have lost their O_2 ligand (ESI voltage 2.8 kV, Figure 4A,C), just like in the nanoESI mass spectra of Figure 2. When raising the capillary voltage to 5.0 kV the peak maximum shifts by 32 Da, corresponding to the incorporation of two oxygen atoms (Figure 4B,D). Clearly, this mass shift is *not* due to the preservation of protein-heme···O_2 interactions in the gas phase. Instead, the +32 Da ions in Figure 4B arise from protein oxidative modifications caused by $^{\bullet}OH$ as the ESI source begins to operate under corona discharge conditions.[63−65] A close-up view of the protein signal also reveals the presence of +16 Da and +48 Da signals (Figure 4C,D), consistent with the fact that the incorporation of single oxygen atoms into amino acid side

DOI: 10.1021/acs.analchem.5b02506
Anal. Chem. 2015, 87, 9538−9545

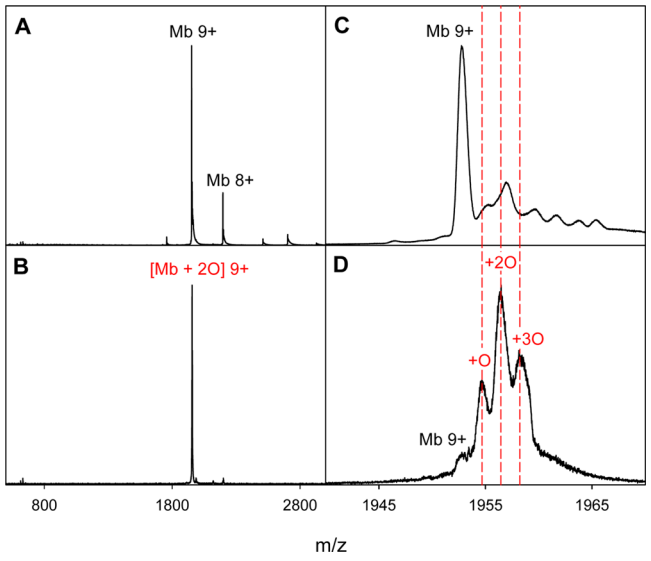

Figure 4. (A, B) Mass spectral data obtained for a MbO_2 sample under regular ESI conditions (capillary voltage 2.8 kV). (B, D) Data obtained for the same sample at an elevated capillary voltage of 5.0 kV. Panels C and D represent close-ups of the base peak signals. In panel D, multiple +16 Da oxygen covalent modifications are annotated as + O, + 2O, and + 3O.

chains is the most commonly observed type of •OH-mediated modification.[68]

It has previously been noted that oxidative modifications can sometimes be induced without raising the ESI voltage, e.g., when corrosion of the stainless steel emitter creates surface irregularities that promote an early onset of corona discharge.[63] It cannot be decided with certainty whether oxidation artifacts of the type discussed here are responsible for the formation of Mb + 32 Da ions in ref 66. In our view such a scenario is quite likely, although differences in the instrumentation used leave room for alternative interpretations.

ESI-MS Analysis of Hb–Ligand Interactions. The experiments discussed above on the three Mb derivatives yielded mixed results; near-complete ligand retention was observed for MbCN, whereas complete dissociation took place for MbCO and MbO_2. It is of interest to compare these findings with data obtained for Hb.

NanoESI mass spectra of HbCN, HbCO, and HbO_2 acquired in positive ion mode are dominated by signals corresponding to the canonical $\alpha_2\beta_2$ quaternary structure, with 18+ being the most intense charge state (Figure 5A–C). A close-up view of the HbCN 18+ signal reveals a complex pattern (Figure 5D). The lower mass range is dominated by Hb carrying 3 or 4 CN^-. Less intense signals are observed for the doubly and singly cyanide bound forms. Similar to the Mb data of Figure 2, it can thus be concluded that HbCN largely survives under ESI-MS conditions. The peak intensity distribution in Figure 5D

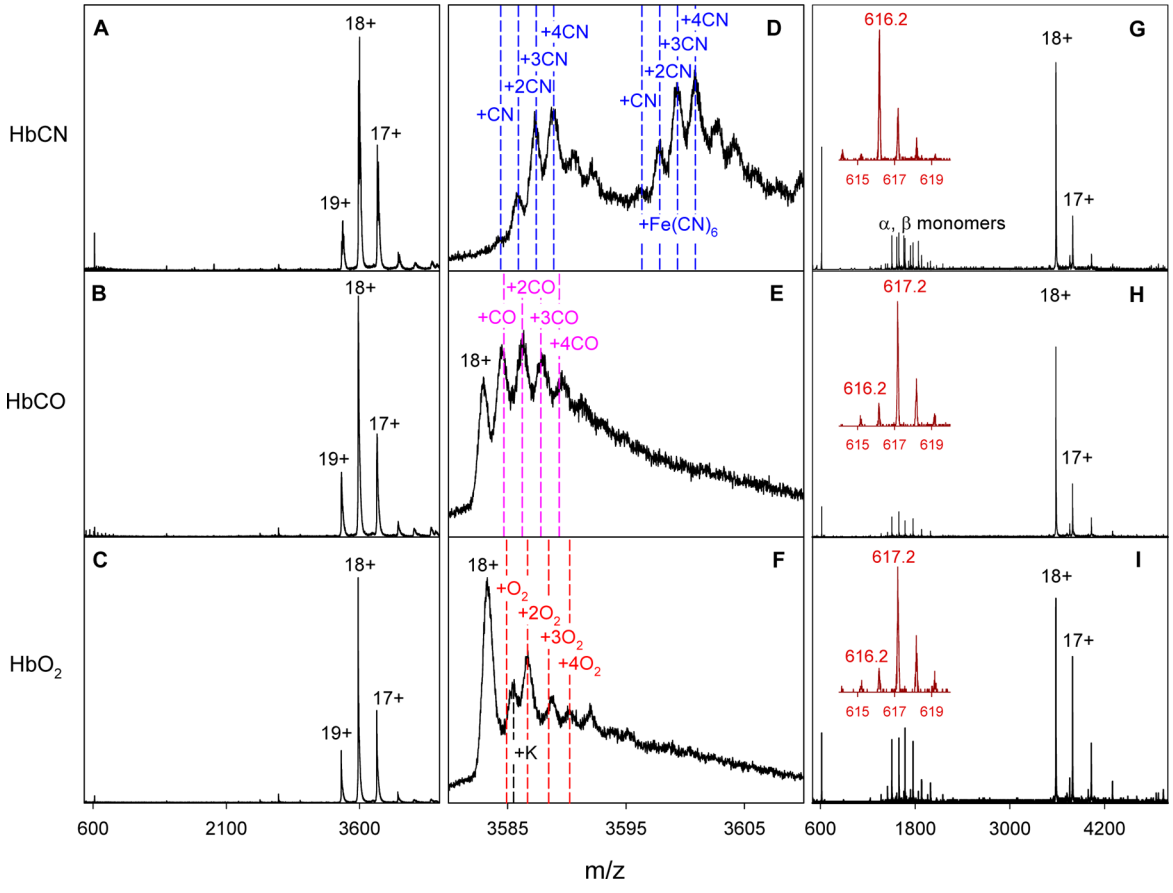

Figure 5. Mass spectra obtained in positive ion mode by exposing Fe^{III} HbCN (first row), Fe^{II} HbCO (middle row), and Fe^{II} HbO_2 (bottom row) to nanoESI conditions. (A–C) Complete spectra, (D,E) close-ups of the 18+ region. Panels G–I show tandem mass spectra, obtained by using the most intense 18+ species as precursor ions, i.e., Hb carrying 4CN (G), Hb carrying 2CO (H), and Hb carrying no ligand (I). Insets in panels G–I zoom in on the heme region. Hb 17+ signals in panels G–I are charge reduced species, likely formed by proton loss during collisional activation.[79]

DOI: 10.1021/acs.analchem.5b02506
Anal. Chem. 2015, 87, 9538–9545

suggests that cyanide loss is on the order of 20%, considering that the protein in bulk solution was fully saturated (Figure 1). Figure 5D also shows a second group of peaks at higher mass. These signals display roughly the same cyanide binding pattern, while additionally carrying a $Fe(CN)_6^{2-(or\ 3-)}$ moiety. This adduct is a remnant of the ferricyanide that was added to the solution for Hb → metHb conversion (see Experimental Section). It is known that Hb in solution can accommodate $Fe(CN)_6^{2-}$ in its organophosphate binding site,[21,37,69] such that the presence of this adduct likely reflects a specific interaction rather than an ESI artifact.

NanoESI of HbCO yields ions that carry between zero and four CO moieties (Figure 5E). The optical spectra of Figure 1B confirm that the HbCO samples used here were fully saturated prior to ESI. Similar to the HbCN experiments, the observation of a heterogeneous CO binding distribution thus implies that some ligand dissociation takes place. The extent of CO loss from HbCO is around 50%. The partial survival of CO-bound Hb in the gas phase is nonetheless remarkable, considering that complete loss of ligand takes place in the corresponding Mb experiments (Figure 2E).

The nanoESI mass spectrum of HbO_2 is dominated by ligand-free protein (Figure 5F). Thus, extensive oxygen loss takes place under ESI-MS conditions, similar to the behavior seen for MbO_2 (Figures 2F and 4F). However, the Hb spectrum in Figure 5F shows a number of adduct peaks. Of particular interest are signals that correspond to +64 Da and +128 Da mass shifts relative to free Hb. In addition, the spectra show a K^+ adduct as well as other low intensity signals of uncertain origin. It is an intriguing question whether the +64 Da and +128 Da adducts correspond to O_2-bound gas phase ions that are remnants of HbO_2 in solution. Gentle collisional activation dramatically reduces the relative intensity of the adduct peaks (Figure 6C). This behavior confirms that the adduct signals, in particular the +64 and +128 Da peaks, are due to weakly bound ligands rather than covalent oxidation artifacts. Thus, our data are consistent with the view that the +64 Da signals in Figures 5F and 6C indeed correspond to $[Hb + 2O_2]^{18+}$, while the +128 Da peak represents $[Hb + 4O_2]^{18+}$. In a similar fashion, collisional activation induces CO loss from electrosprayed HbCO and dissociation of HCN from HbCN (Figure 6A,B).

In summary, the Hb experiments of this work show that under properly optimized ESI-MS conditions HbCN largely retains its bound ligands, while HbCO undergoes ~50% ligand loss. For HbO_2 it appears that a small fraction (<10%) of the bound molecular oxygen can be retained after ESI. This ligand retention trend in the gas phase is qualitatively consistent with the Hb binding affinity of the three ligands in solution.[21,24]

Complete Hb tandem mass spectra are depicted in Figure 5G–I, using the most intense ions of Figure 5A–C as precursors. Dissociation of the $\alpha_2\beta_2$ complexes proceeds with asymmetric charge partitioning, generating highly charged monomers and charge-depleted trimers. This behavior is consistent with earlier dissociation experiments on Hb[70] and other multiprotein assemblies.[4] Not surprisingly, the Fe^{III} heme in HbCN remains unaffected under positive ion conditions, evident from the m/z 616.2 product ion signal (Figure 5G). For the HbCO and HbO_2 samples, the heme region is dominated by Fe^{II} heme with m/z 617.2 (Figure 5H,I). In addition, these two samples show a low level of Fe^{III} heme (~15%, m/z 616.2). This implies that electrochemical oxidation of ferrous heme during positive ion nanoESI is less pronounced for Hb than in the case of Mb (Figure 2H,I). We attribute this difference to the higher molar concentration of heme in the Hb samples.

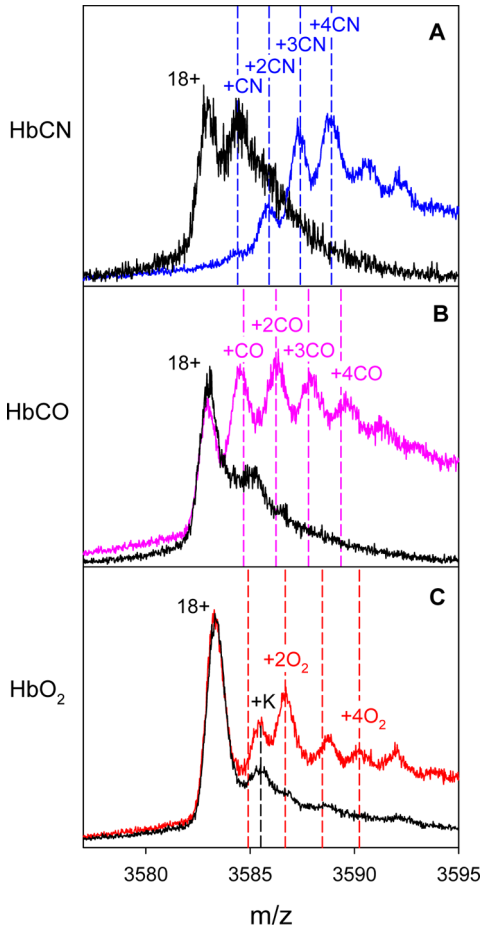

Figure 6. Close-up views of the 18+ region for (A) HbCN, (B) HbCO, and (C) HbO_2 samples acquired under gentle ESI conditions (colored spectra) and with collisional activation (black lines). Neutral loss events shift the peak envelopes to lower m/z in all three cases. Data in panels A and B were obtained in MS/MS mode by locking the quadrupole on the 4CN and 2CO peak maxima, respectively. In panel C, activation was achieved by raising the cone voltage from 5 to 60 V without precursor ion selection.

MS analyses on the three Hb derivatives were also conducted in negative ion mode. Unfortunately, the spectra obtained under those conditions exhibited low S/N ratios. However, there was no evidence for enhanced ligand retention in negative ion mode compared to the positive ion spectra of Figure 5 (data not shown).

CONCLUSIONS

The retention of protein–ligand interactions in the gas phase has been demonstrated for countless systems.[2−7,9−15] Surprisingly, the previous ESI-MS literature has largely bypassed the binding of physiologically relevant low molecular weight ligands to heme proteins. Here we demonstrate for the first time that MbCN and HbCO can be successfully transferred into the vacuum of a mass spectrometer. Our experiments also suggest that partial oxygen retention is possible for HbO_2. In addition we confirm that it is possible for HbCN to survive the ESI process.[37] Complete ligand loss is observed for MbCO and MbO_2. The latter finding contrasts an earlier study that reported partial O_2 retention for MbO_2.[66] The origin of this

DOI: 10.1021/acs.analchem.5b02506
Anal. Chem. 2015, 87, 9538−9545

discrepancy remains uncertain, but our experiments suggest that the oxygen-bound Mb observed in ref 66 may have been a covalently bound artifact generated under corona discharge conditions.

The current work was partly motivated by the question whether changes in heme oxidation state are a contributing factor for the disruption of globin−ligand interactions during ESI. In agreement with earlier studies,[44,59,60] we confirm the occurrence of such redox processes. However, comparative experiments in positive and negative ion mode reveal that this factor is not the root cause of CO and O_2 dissociation from globins under ESI-MS conditions.

It is surprising that gaseous Mb is more prone to ligand loss than Hb. The origin of this behavior is not clear, but it is possible that the major conformational changes taking place for Hb during binding (a 15° rotation of the two $\alpha\beta$ units relative to each other[26]) play a role in this context. This Hb conformational switching is in contrast to Mb which has a conformation that remains largely unaltered upon binding.[71] In addition, one has to consider the 4-fold difference in size (and mass) between Hb and Mb which will affect the interplay between collisional excitation and collisional cooling in the ion sampling interface.[72] The lower number of vibrational degrees of freedom in Mb is another factor that may enhance the efficiency of collision-induced ligand loss.[73,74]

Under ideal conditions, ESI-MS titration experiments can provide direct insights into the nature of cooperative protein interactions by measuring the full distributions of bound ligands.[75] Obtaining such information for Hb would be of particular importance for addressing open questions related to allosteric binding.[25,26,30] Unfortunately, the ligand distributions of Figure 5D−F cannot directly serve this purpose because even for the two most favorable cases (HbCN and HbCO) there still is a rather noticeable ligand fraction that dissociates prior to detection.

The structural characterization of protein ions in the gas phase remains a difficult task. In recent years, various spectroscopic techniques have emerged that can help address this issue.[76−78] Condensed phase experiments have abundantly demonstrated that heme−protein interactions give rise to spectroscopic signatures that offer a unique opportunity for interrogating conformational properties of the heme binding pocket. Of central importance for these condensed phase studies is the possibility to modulate the heme spectroscopic properties via the choice of ligand, e.g., by comparing deoxy, CN^-, CO, and O_2 derivatives.[21,25−30,54] The successful detection of various ligand-bound globin states in the present ESI-MS study suggests that it may be possible to extend such spectroscopic investigations to gaseous globin ions. It is hoped that the current work will set the stage for future ventures of this kind.

AUTHOR INFORMATION

Corresponding Author

*E-mail: konerman@uwo.ca.

Notes

The authors declare no competing financial interest.

ACKNOWLEDGMENTS

This work was supported by the Natural Sciences and Engineering Research Council of Canada. We thank Prof. Martin Stillman for help with the CO binding experiments and Dr. Siavash Vahidi for critical reading of the manuscript.

REFERENCES

(1) Fenn, J. B. *Angew. Chem., Int. Ed.* **2003**, *42*, 3871−3894.
(2) Ganem, B.; Li, Y.-T.; Henion, J. D. *J. Am. Chem. Soc.* **1991**, *113*, 7818−7819.
(3) Lössl, P.; Snijder, J.; Heck, A. J. R. *J. Am. Soc. Mass Spectrom.* **2014**, *25*, 906−917.
(4) Benesch, J. L. P.; Ruotolo, B. T.; Simmons, D. A.; Robinson, C. V. *Chem. Rev.* **2007**, *107*, 3544−3567.
(5) Loo, J. A. *Int. J. Mass Spectrom.* **2000**, *200*, 175−186.
(6) Sharon, M. *J. Am. Soc. Mass Spectrom.* **2010**, *21*, 487−500.
(7) Benesch, J. L. P.; Ruotolo, B. T. *Curr. Opin. Struct. Biol.* **2011**, *21*, 641−649.
(8) Wilm, M.; Mann, M. *Anal. Chem.* **1996**, *68*, 1−8.
(9) Liu, L.; Baergen, A.; Michelsen, K.; Kitova, E. A.; Schnier, P. D.; Klassen, J. S. *J. Am. Soc. Mass Spectrom.* **2014**, *25*, 742−750.
(10) Zhou, M.; Jones, C. M.; Wysocki, V. H. *Anal. Chem.* **2013**, *85*, 8262−8267.
(11) Schennach, M.; Breuker, K. *J. Am. Soc. Mass Spectrom.* **2015**, *26*, 1059−1067.
(12) Lermyte, F.; Williams, J. P.; Brown, J. M.; Martin, E. M.; Sobott, F. *J. Am. Soc. Mass Spectrom.* **2015**, *26*, 1068−1076.
(13) Hogan, C. J.; Ruotolo, B. T.; Robinson, C. V.; de la Mora, J. F. *J. Phys. Chem. B* **2011**, *115*, 3614−3621.
(14) Wyttenbach, T.; Pierson, N. A.; Clemmer, D. E.; Bowers, M. T. *Annu. Rev. Phys. Chem.* **2014**, *65*, 175−196.
(15) Young, L. M.; Saunders, J. C.; Mahood, R. A.; Revill, C. H.; Foster, R. J.; Tu, L.-H.; Raleigh, D. P.; Radford, S. E.; Ashcroft, A. E. *Nat. Chem.* **2014**, *7*, 73−81.
(16) Bich, C.; Baer, S.; Jecklin, M. C.; Zenobi, R. *J. Am. Soc. Mass Spectrom.* **2010**, *21*, 286−289.
(17) Kitova, E. N.; El-Hawiet, A.; Schnier, P. D.; Klassen, J. S. *J. Am. Soc. Mass Spectrom.* **2012**, *23*, 431−441.
(18) Daniel, J. M.; Friess, S. D.; Rajagopalan, S.; Wendt, S.; Zenobi, R. *Int. J. Mass Spectrom.* **2002**, *216*, 1−27.
(19) Peschke, M.; Verkerk, U. H.; Kebarle, P. *J. Am. Soc. Mass Spectrom.* **2004**, *15*, 1424−1434.
(20) Dickerson, R. E.; Geis, I. *Hemoglobin: Structure, Function, Evolution, and Pathology*; The Benjamin/Cummings Publishing Company, Inc.: Menlo Park, CA, 1983.
(21) Antonini, E.; Brunori, M. *Hemoglobin and Myoglobin in Their Reactions With Ligands*; North-Holland Publishing Company: Amsterdam, The Netherlands, 1971.
(22) Degtyarenko, I.; Biarnes, X.; Nieminen, R. M.; Rovira, C. *Coord. Chem. Rev.* **2008**, *252*, 1497−1513.
(23) Sigfridsson, E.; Ryde, U. *JBIC, J. Biol. Inorg. Chem.* **1999**, *4*, 99−110.
(24) Olson, J. S.; Phillips, G. N., Jr. *JBIC, J. Biol. Inorg. Chem.* **1997**, *2*, 544−552.
(25) Ackers, G. K.; Doyle, M. L.; Myers, D.; Daugherty, M. A. *Science* **1992**, *255*, 54−63.
(26) Eaton, W. A.; Henry, E. R.; Hofrichter, J.; Mozzarelli, A. *Nat. Struct. Biol.* **1999**, *6*, 351−358.
(27) Lukin, J. A.; Ho, C. *Chem. Rev.* **2004**, *104*, 1219−1230.
(28) Perutz, M. F.; Wilkinson, A. J.; Paoli, M.; Dodson, G. G. *Annu. Rev. Biophys. Biomol. Struct.* **1998**, *27*, 1−34.
(29) Englander, J. J.; Del Mar, C.; Li, W.; Englander, S. W.; Kim, J. S.; Stranz, D. D.; Hamuro, Y.; Woods, V. L. *Proc. Natl. Acad. Sci. U. S. A.* **2003**, *100*, 7057−7062.
(30) Bellelli, A.; Brunori, M. *Biochim. Biophys. Acta, Bioenerg.* **2011**, *1807*, 1262−1272.
(31) Reed, C. A.; Cheung, S. K. *Proc. Natl. Acad. Sci. U. S. A.* **1977**, *74*, 1780−1784.
(32) Wilson, S. A.; Green, E.; Mathews, II; Benfatto, M.; Hodgson, K. O.; Hedman, B.; Sarangi, R. *Proc. Natl. Acad. Sci. U. S. A.* **2013**, *110*, 16333−16338.

DOI: 10.1021/acs.analchem.5b02506
Anal. Chem. 2015, 87, 9538−9545

(33) Rovira, C.; Schulze, B.; Eichinger, M.; Evanseck, J. D.; Parrinello, M. *Biophys. J.* **2001**, *81*, 435−445.
(34) Aranda, R., IV; Cai, H.; Worley, C. E.; Levin, E. J.; Li, R.; Olson, J. S.; Phillips, G. N., Jr; Richard, M. P. *Proteins: Struct., Funct., Genet.* **2009**, *75*, 217−230.
(35) Ernst, A.; Zibrak, J. D. *N. Engl. J. Med.* **1998**, *339*, 1603−1608.
(36) Robinson, V. L.; Smith, B. B.; Arnone, A. *Biochemistry* **2003**, *42*, 10113−10125.
(37) Boys, B. L.; Kuprowski, M. C.; Konermann, L. *Biochemistry* **2007**, *46*, 10675−10684.
(38) Arcovito, A.; Benfatto, M.; Cianci, M.; Hasnain, S. S.; Nienhaus, K.; Nienhaus, G. U.; Savino, C.; Strange, R. W.; Vallone, B.; Della Longa, S. *Proc. Natl. Acad. Sci. U. S. A.* **2007**, *104*, 6211−6216.
(39) Maurus, R.; Overall, C. M.; Bogumil, R.; Luo, Y.; Mauk, A. G.; Smith, M.; Brayer, G. D. *Biochim. Biophys. Acta, Protein Struct. Mol. Enzymol.* **1997**, *1341*, 1−13.
(40) McLendon, G.; Sandberg, K. *J. Biol. Chem.* **1978**, *253*, 3913−3917.
(41) Fersht, A. R. *Structure and Mechanism in Protein Science*; W. H. Freeman & Co.: New York, 1999.
(42) Katta, V.; Chait, B. T. *J. Am. Chem. Soc.* **1991**, *113*, 8534−8535.
(43) Tiedemann, M. T.; Heinrichs, D. E.; Stillman, M. J. *J. Am. Chem. Soc.* **2012**, *134*, 16578−16585.
(44) Mark, K. J.; Douglas, D. J. *Rapid Commun. Mass Spectrom.* **2006**, *20*, 111−117.
(45) Dobo, A.; Kaltashov, I. A. *Anal. Chem.* **2001**, *73*, 4763−4773.
(46) Gross, D. S.; Zhao, Y.; Williams, E. R. *J. Am. Soc. Mass Spectrom.* **1997**, *8*, 519−524.
(47) Schmidt, A.; Karas, M. *J. Am. Soc. Mass Spectrom.* **2001**, *12*, 1092−1098.
(48) Enyenihi, A. A.; Yang, H.; Ytterberg, A. J.; Lyutvinskiy, Y.; Zubarev, A. R. *J. Am. Soc. Mass Spectrom.* **2011**, *22*, 1763−1770.
(49) Kang, Y.; Terrier, P.; Douglas, D. J. *J. Am. Soc. Mass Spectrom.* **2011**, *22*, 290−299.
(50) Griffith, W. P.; Kaltashov, I. A. *Biochemistry* **2003**, *42*, 10024−10033.
(51) Light-Wahl, K. J.; Schwartz, B. L.; Smith, R. D. *J. Am. Chem. Soc.* **1994**, *116*, 5271−5278.
(52) Green, B. N.; Vinogradov, S. N. *J. Am. Soc. Mass Spectrom.* **2004**, *15*, 22−27.
(53) Scarff, C. A.; Patel, V. J.; Thalassinos, K.; Scrivens, J. H. *J. Am. Soc. Mass Spectrom.* **2009**, *20*, 625−631.
(54) Schweitzer-Stenner, R.; Cupane, A.; Leone, M.; Lemke, C.; Schott, J.; Dreybrodt, W. *J. Phys. Chem. B* **2000**, *104*, 4754−4764.
(55) Falvo, C.; Daniault, L.; Vieille, T.; Kemlin, V.; Lambry, J. C.; Meier, C.; Vos, M. H.; Bonvalet, A.; Joffre, M. *J. Phys. Chem. Lett.* **2015**, *6*, 2216−2222.
(56) Van Berkel, G. J.; Kertesz, V. *Anal. Chem.* **2007**, *79*, 5510−5520.
(57) Pozniak, B. P.; Cole, R. B. *J. Am. Soc. Mass Spectrom.* **2015**, *26*, 369−385.
(58) Kebarle, P.; Verkerk, U. H. *Mass Spectrom. Rev.* **2009**, *28*, 898−917.
(59) Wells, J. M.; Reid, G. E.; Engel, B. J.; Pan, P.; McLuckey, S. A. *J. Am. Soc. Mass Spectrom.* **2001**, *12*, 873−876.
(60) He, F.; Hendrickson, C. L.; Marshall, A. G. *J. Am. Soc. Mass Spectrom.* **2000**, *11*, 120−126.
(61) Bateman, K. P. *J. Am. Soc. Mass Spectrom.* **1999**, *10*, 309−317.
(62) Nemes, P.; Marginean, I.; Vertes, A. *Anal. Chem.* **2007**, *79*, 3105−3116.
(63) Chen, M.; Cook, K. D. *Anal. Chem.* **2007**, *79*, 2031−3036.
(64) Boys, B. L.; Kuprowski, M. C.; Noël, J. J.; Konermann, L. *Anal. Chem.* **2009**, *81*, 4027−4034.
(65) Maleknia, S. D.; Downard, K. *Mass Spectrom. Rev.* **2001**, *20*, 388−401.
(66) Konishi, Y.; Feng, R. *Biochemistry* **1994**, *33*, 9706−9711.
(67) Sowole, M. A.; Konermann, L. *Anal. Chem.* **2014**, *86*, 6715−6722.
(68) Xu, G.; Chance, M. R. *Chem. Rev.* **2007**, *107*, 3514−3543.
(69) Sen, U.; Dasgupta, J.; Choudhury, D.; Datta, P.; Chakrabarti, A.; Chakrabarty, S. B.; Chakrabarty, A.; Dattagupta, J. K. *Biochemistry* **2004**, *43*, 12477−12488.
(70) Abzalimov, R. R.; Frimpong, A. K.; Kaltashov, I. A. *Int. J. Mass Spectrom.* **2006**, *253*, 207−216.
(71) Phillips, S. E. V. *J. Mol. Biol.* **1980**, *142*, 531−554.
(72) Chernushevich, I. V.; Thomson, B. A. *Anal. Chem.* **2004**, *76*, 1754−1760.
(73) Marzluff, E. M.; Campbell, S.; Rodgers, M. T.; Beauchamp, J. L. *J. Am. Chem. Soc.* **1994**, *116*, 6947−6948.
(74) Laskin, J.; Futrell, J. H. *Mass Spectrom. Rev.* **2003**, *22*, 158−181.
(75) Dyachenko, A.; Gruber, R.; Shimon, L.; Horovitz, A.; Sharon, M. *Proc. Natl. Acad. Sci. U. S. A.* **2013**, *110*, 7235−7239.
(76) Talbot, F. O.; Rullo, A.; Yao, H.; Jockusch, R. A. *J. Am. Chem. Soc.* **2010**, *132*, 16156−16164.
(77) Polfer, N. C.; Oomens, J. *Phys. Chem. Chem. Phys.* **2007**, *9*, 3804−3817.
(78) Nagornova, N. S.; Guglielmi, M.; Doemer, M.; Tavernelli, I.; Rothlisberger, U.; Rizzo, T. R.; Boyarkin, O. V. *Angew. Chem., Int. Ed.* **2011**, *50*, 5383−5386.
(79) Freeke, J.; Bush, M. F.; Robinson, C. V.; Ruotolo, B. T. *Chem. Phys. Lett.* **2012**, *524*, 1−9.

DOI: 10.1021/acs.analchem.5b02506
Anal. Chem. 2015, 87, 9538−9545